Published in final edited form as:
Drug Metab Dispos. 2008 May ; 36(5): 963–970. doi:10.1124/dmd.107.018960.

CYP1B1 Is Not a Major Determinant of the Disposition of Aromatase Inhibitors in Epithelial Cells of Invasive Ductal Carcinoma

Mostafizur Rahman, **Sigurd F. Lax**, **Carrie H. Sutter**, **Quynh T. Tran**, **Gaylene L. Stevens**, **Gary L. Emmert**, **Jose Russo**, **Richard J. Santen**, and **Thomas R. Sutter**

W. Harry Feinstone Center for Genomic Research (M.R., C.H.S., Q.T.T., G.L.S., T.R.S.) and Departments of Chemistry (M.R., G.L.E., T.R.S.) and Biology (M.R., C.H.S., Q.T.T., G.L.S., T.R.S.), University of Memphis, Memphis, Tennessee; Department of Pathology, General Hospital Graz West, Graz, Austria (S.F.L.); Fox Chase Cancer Center, Philadelphia, Pennsylvania (J.R.); and School of Medicine, University of Virginia, Charlottesville, Virginia (R.J.S.)

Abstract

CYP1B1 and CYP19 (aromatase) have been shown to be expressed in breast tumors. Both enzymes are efficient estrogen hydroxylases, indicating the potential for overlapping substrate and inhibitor specificity. We measured the inhibition properties of aromatase inhibitors (AIs) against CYP1B1-catalyzed hydroxylation of 17β-estradiol (E2) to determine whether CYP1B1 affects the disposition of AIs. In addition, we estimated the frequency of coexpression of these enzymes in breast tumor epithelium. Immunohistochemical analyses of CYP19 and CYP1B1 in a panel of 29 cases of invasive ductal carcinoma of the breast showed epithelial cell staining for CYP19 in 76% and for CYP1B1 in 97% of the samples. Statistical analysis showed no significant correlation (0.33) for positive expression of CYP19 and CYP1B1 ($p > 0.07$). CYP1B1 inhibition was determined for two steroidal inhibitors: formestane and exemestane and five nonsteroidal inhibitors: aminoglutethimide, fadrozole, anastrozole, letrozole, and vorozole. Of the seven compounds tested, only vorozole exhibited inhibition of CYP1B1 activity with IC_{50} values of 17 and 21 μM for 4-hydroxy estradiol and 2-hydroxy estradiol, respectively. The estimated K_i values of vorozole for E2 4- and 2-hydroxylation were 7.26 and 6.84 μM, respectively. Spectrophotometric studies showed that vorozole was a type II inhibitor of CYP1B1. This study shows that with the exception of vorozole, the aromatase inhibitors are selective for CYP19 relative to CYP1B1. Thus, although both CYP19 and CYP1B1 are expressed in a high percentage of breast cancers, CYP1B1 is not a major determinant of the disposition of AIs.

CYP19 (aromatase) catalyzes the formation of the phenolic A ring of estrogens, converting androstenedione to estrone and testosterone to estradiol (Johnston and Dowsett, 2003). CYP19 is found in glandular and nonglandular tissues, including adrenal glands, ovaries, placenta, testes, adipose tissue, muscle, brain, normal breast, and breast cancer tissue. Important to this work, studies have shown that substantial levels of estrogens arise from aromatase activity in breast tissue (Miller, 1991; Bulun et al., 1993). CYP19 protein and activity have been detected in both the epithelial cells and surrounding stroma and adipose tissue of breast tumors (Esteban et al., 1992; Lu et al., 1996; Brodie et al., 1997; Oliveira et al., 2006; Miki et al., 2007). A recent study showed that although significant CYP19 immunoreactivity occurred in each of

Address correspondence to: Dr. Thomas R. Sutter, W. Harry Feinstone Center for Genomic Research, University of Memphis, 201 Life Sciences Building, Memphis, TN 38152. E-mail: tsutter@memphis.edu.

Article, publication date, and citation information can be found at http://dmd.aspetjournals.org.

these cellular compartments of breast tumors, a significant positive correlation between biochemical activity and immunostaining was detected only for the epithelium (Sasano et al., 2005).

Aromatase inhibitors (AIs) are drugs that inhibit CYP19, preventing the formation of estrogens. The AIs are subdivided into steroidal (type I) and nonsteroidal (type II) agents (Johnston and Dowsett, 2003; Miller, 2006). Type 1 agents are analogs of androgens that bind to CYP19 through either reversible or irreversible mechanisms, competing with the natural substrates. Type II inhibitors reversibly interact with the heme iron of cytochrome P450 (Miller, 2006). AIs are also categorized as 1st, 2nd, and 3rd generation inhibitors based on their chronological order of clinical development (Johnston and Dowsett, 2003). AI therapy has been shown to be effective in the prevention of new and recurrent breast cancer in women previously treated for an estrogen receptor-positive tumor. At present, 3rd generation AIs developed in the early 1990s have been introduced into the treatment of estrogen receptor-positive breast cancer in the metastatic, as well as the adjuvant settings (Joensuu et al., 2005).

CYP1B1, an extrahepatic enzyme, is the third member of the CYP1 family and is the only known member of CYP1B subfamily (Sutter et al., 1994). It is expressed constitutively in many human tissues, including breast and ovary (Shimada et al., 1996; Jefcoate et al., 2000; Muskhelishvili et al., 2001). CYP1B1 is the most catalytically efficient 17β-estradiol (E2) hydroxylase, preferentially producing 4-hydroxy-E2 (Hayes et al., 1996). Furthermore, CYP1B1 can oxidize the catechol estrogens to the chemically reactive semiquinone and quinone intermediates that form DNA adducts that can initiate breast, prostate, and other types of cancer (Cavalieri et al., 2006). Increased E2 4-hydroxylase activity has been measured in human breast cancer compared with normal breast tissue (Liehr and Ricci, 1996), and increased expression of CYP1B1 protein has been shown to occur in several types of human cancers, including breast and ovary (McFadyen et al., 1999).

Expression of CYP19 (Esteban et al., 1992; Brodie et al., 1997; Sasano et al., 2005; Oliveira et al., 2006; Miki et al., 2007) and CYP1B1 (McFadyen et al., 1999) proteins has been detected in breast cancer independently by immunohistochemistry, indicating that these enzymes are major tumor forms of cytochrome P450 expressed in breast tumors. In addition, higher expression of CYP19 and CYP1B1 mRNAs has also been reported in breast cancer tissues compared with normal tissues (Singh et al., 2005), suggesting the importance of these two enzymes in the development and progression of breast cancer. Both CYP1B1 and CYP19 are efficient E2 hydroxylases (Aoyama et al., 1990; Hayes et al., 1996; Liehr and Ricci, 1996; Jefcoate et al., 2000; Singh et al., 2005), indicating the potential for overlapping substrate and inhibitor specificity. To determine whether CYP1B1 can affect the disposition of AIs, we measured the inhibition properties of a series of AIs against CYP1B1-catalyzed hydroxylation of E2. In addition, the frequency of coexpression of these enzymes in breast tumor epithelium was estimated.

Materials and Methods

Materials

Human CYP19 and human CYP1B1 microsomes were purchased from BD Gentest (Woburn, MA). The AIs obtained from multiple sources were kindly provided by Dr. William R. Miller (Western General Hospital, University of Edinburgh, Edinburgh, UK). Formestane, letrozole, fadrozole, and aminoglutethimide were obtained from Novartis (Basel, Switzerland). Exemestane was obtained from Pfizer (New York, NY). Anastrozole was obtained from AstraZeneca Pharmaceuticals LP (Wilmington, DE), and vorozole was from Jannsen (Beerse, Belgium). The other materials used in this study were described previously in detail (Rahman et al., 2006).

CYP19 Protein Expression and Purification of Hexahistidine-Tagged Proteins in *Escherichia coli*

To generate fusion proteins, cDNA constructs were cloned into a vector engineered such that the expressed protein has an amino-terminal hexahistidine peptide tag to allow purification by metal chelate affinity chromatography. For the human CYP19 expression construct (herein referred to as His_6-CYP19), a 730-bp PstI-KpnI fragment of the human aromatase cDNA (nucleotide positions 395–1125) (Corbin et al., 1988) was subcloned into the PstI-KpnI site of vector pTrcHis C (Invitrogen, Carlsbad, CA) and transformed into *E. coli* JM 109 cells. The cDNA orientation and reading frame were verified by DNA sequence analysis.

E. coli expression and purification followed our previously published methods (Walker et al., 1998). *E. coli*, transformed with His_6-CYP19 plasmid, were inoculated into 5 ml of Terrific broth [1.2% (w/v) bacto-tryptone, 2.4% (w/v) bacto-yeast extract, 0.4% (v/v) glycerol, 17 mM KH_2PO_4, 72 mM K_2HPO_4] containing 100 μg/ml ampicillin (Terrific broth + ampicillin), and grown overnight at 37°C at 200 rpm. The overnight culture (5 ml) was inoculated into 200 ml of (His_6-CYP19) Terrific broth + ampicillin and grown at 37°C with vigorous shaking for about 2.5 h until the cells were in midlog phase (A_{600} = 0.6–0.8). To induce protein expression, isopropyl β-D-thiogalactoside was added to a final concentration of 1 mM, followed by incubation for 5 h at 37°C. A 0.5-ml cell sample was pelleted by centrifugation, resuspended, and boiled for 5 min in 100 μl of SDS sample dilution buffer (50 mM Tris.Cl, pH 6.8, 1.5% 2-mercaptoethanol, 2% SDS, 0.1% bromophenol blue, 10% glycerol). Fifteen microliters of this cell lysate was analyzed by SDS-polyacrylamide gel electrophoresis (PAGE) to confirm induction of the 35-kDa His_6-CYP19 protein.

The induced *E. coli* culture (200 ml) was pelleted by centrifugation at 5000*g* for 10 min at 4° C. The cells were resuspended and lysed in 6 M guanidinium hydrochloride, 100 mM sodium phosphate, 10 mM Tris.Cl, pH 8.0, and the hexahistidine-tagged protein was purified by affinity column chromatography with nitrilotriacetic acid-agarose (QIAGEN, Valencia, CA). Elution of His_6-CYP19 from the nitrilotriacetic acid-agarose was achieved using a pH step gradient (pH 8.0, 6.3, and 4.5). Approximately 1 mg of affinity purified protein was then separated by SDS-PAGE using a 20-cm-long 12% polyacrylamide gel and stained with 0.3 M $CuCl_2$ for 5 min. The area of the gel containing the fusion protein was excised using a razor blade and destained by repeated washing in 0.25 M EDTA and 0.25 M Tris.Cl, pH 9.0. The protein was eluted from the gel slice by electroelution in 25 mM Tris base and 192 mM glycine, pH 8.8, containing 0.01% SDS, then dialyzed against 0.5× phosphate-buffered saline and frozen at −20°C. The purity of the electroeluted protein was confirmed by Coomassie stain of the protein analyzed by SDS-PAGE.

Generation of Polyclonal Antibodies

All animal procedures were carried out by Spring Valley Laboratories (Sykesville, MD). A polyacrylamide gel slice containing 250 μg of purified fusion protein was minced and emulsified in complete Freund's adjuvant and used for primary s.c. immunization of New Zealand White male rabbits. Rabbits were boosted 2 and 4 weeks following the primary immunization with 200 μg of purified protein, emulsified in incomplete Freund's adjuvant. Serum was prepared from blood taken 5 weeks following the primary immunization. The serum IgG was purified by protein A affinity purification (Pierce Chemical, Rockford, IL; Walker et al., 1998).

Immunoblot Analysis

Microsomal samples were solubilized in SDS sample dilution buffer and separated by denaturing SDS-PAGE. Separated proteins were transferred to nitrocellulose (Hybond ECL; GE Healthcare, Little Chalfont, Buckinghamshire, UK) and incubated with primary antibody

(anti-CYP19 at 5 μg/ml purified IgG and anti-CYP1B1 (at 10 μg/ml; Walker et al., 1998) for 1 h at room temperature. Bound antibody was detected by incubation for 1 h with a horseradish peroxidase-linked secondary antibody (goat anti-rabbit IgG, 1:30,000 dilution; Promega, Madison, WI). Bound secondary antibody was detected by an enhanced chemiluminescence method according to the manufacturer's instructions (Pierce).

Immunohistochemical Analysis

The purified serum IgG was used at a concentration of either 10 μg/ml (CYP19) or 10 μg/ml (CYP1B1). Nonspecific staining was assessed using normal rabbit serum (Sigma-Aldrich, St. Louis, MO) at a dilution of 1:5000. Paraffin-embedded human breast cancer samples including 29 cases of invasive ductal carcinoma (IDC), cases of cancer metastasis, and samples of normal breast tissue adjacent to cancer tissue were obtained as tissue microarrays from Imgenex (San Diego, CA; IMH-36460). Imgenex is the U.S. distributor for SuperBioChips (South Korea). Results for staining for estrogen receptor (ER), progesterone receptor (PR), and p53 were provided by Imgenex with the tissue arrays. The source of antibodies for these proteins was Dako Denmark A/S (Glostrup, Denmark; ER, M7047; PR, A0098; p53, M7001). Both the breast and placental tissues were obtained as discarded tissue, without patient identifiers. The slides were deparaffinized in xylene (twice for 4 min) followed by washing in 100% ethanol (4 min), 95% ethanol (2 min), 80% ethanol (15 s), and distilled water. Immunohistochemistry was performed as described previously (Walker et al., 1998), using diaminobenzidine as the chromagen. The slides were washed with distilled water for 1 min and counterstained for 1 min with hematoxylin. The intensities of the immunoreactivity were scored from 0 to 5, and the sample identifications were blinded from the pathologist (J.R.).

Statistical Analysis

Correlations between the epithelial cell expression of aromatase, CYP1B1, ER, PR, and p53 in IDC of the breast were determined using the Pearson χ^2 test.

Inhibition Kinetics Assay Using the Microsomal Fraction Containing Recombinant Human CYP1B1

The recombinant human CYP1B1 protein was expressed in *Saccharomyces cerevisiae* as described previously (Hayes et al., 1996). Specific CYP1B1 protein content was estimated and evaluated by measuring the enzymatic activity as previously described (Rahman et al., 2006). For the initial AI screen, the same preparation of CYP1B1 microsomes was used for the inhibition studies. The measured E2 4-hydroxylase activity was 1.23 nmol/min/nmol P450, consistent with the turnover number published in our previous studies (Hayes et al., 1996; Rahman et al., 2006). The inhibition kinetics of CYP1B1 was determined in a range expected to produce 30 to 90% inhibition. A fixed substrate concentration and varying inhibitor concentrations were used to determine the IC_{50} value at the point where 50% inhibition of the catalytic activity of the enzyme occurred. The E2 hydroxylation assay was performed with the addition of inhibitor and has been previously described in detail (Rahman et al., 2006). Inhibition was calculated as percentage of product formation compared with the corresponding control (enzyme-substrate reaction) without the inhibitors.

To determine the K_i value and type of inhibition from Dixon plots (Dixon, 1953), 10 pmol human CYP1B1 was assayed in the presence of three substrate concentrations: 1, 3, and 5 μM E2, and five concentrations of vorozole: 0.0, 5.0, 10.0, 20.0, and 40.0 μM, respectively. The substrate concentrations were approximately equal to 0.5 × K_m, 2 × K_m, and 4 × K_m. The accurate values were 0.612 (0.5 × K_m), 2.45 (2 × K_m), and 4.89 (4 × K_m) μM. The concentration of vorozole was chosen and varied to give a wide range of percent inhibition based on our previously determined IC_{50} for this inhibitor. Linear regression analyses for each of the three substrate concentrations were plotted on a single graph of 1/rate versus inhibitor concentration.

The rate of product formation was determined as picomoles of product per minute in each reaction. The coordinates of intersection of regression lines in Dixon plots are $-K_i$ and $1/K_{cat}$. The K_i value is determined by averaging the results from individual intersections where the three regression lines did not intersect at a single point. Cornish-Bowden plot (S/V against i) was also constructed using the same data to model the type of inhibition (Cornish-Bowden, 1974).

Binding Difference Spectra of P4501B1 with Vorozole

The binding of vorozole to CYP1B1 was monitored by difference spectroscopy (Schenkman et al., 1967). The P450 content in microsomes containing recombinant human CYP1B1 expressed in the yeast *S. cerevisiae* was estimated to be 217.5 pmol/mg protein on the basis of reduced CO difference spectra. The microsomal protein was suspended in 0.1 M KPO_4 buffer, pH 7.4. The diluted sample was transferred into both sample and reference cuvettes to give a protein concentration of 1 mg/ml, and the baselines of equal light absorbance were recorded using a Varian Cary 100 Bio UV-Visible spectrophotometer (Varian, Inc., Palo Alto, CA) between 350 and 500 nm at ambient temperature. After the baseline had been recorded, vorozole dissolved in dimethyl sulfoxide was added to the sample cuvette in 2-μl aliquots and mixed gently with a pipette into the sample mixture. Vorozole was added to produce final concentrations of 5.0, 20.0, and 80.0 μM. An equal volume of carrier solvent was added to the reference cuvette. The sample was allowed to stand for 1 min, and the difference spectra were determined (350–500 nm) after each addition and graphed with baseline and background correction.

Results

Expression of CYP19 Protein in *E. coli* and Production of Polyclonal Antibodies to CYP19

For the generation of polyclonal antibodies to CYP19, we expressed CYP19 as hexahistidine-tagged fusion proteins in *E. coli*. High expression of His_6-CYP19 was observed in protein extracts of induced *E. coli* cultures (Fig. 1A, lane 2). Metal chelate affinity purification yielded a 35-kDa CYP19 fusion protein, and this was confirmed by SDS-PAGE (Fig. 1A, lanes 4–7). Immunoblot analyses using the anti His_6-CYP19 and anti His_6-CYP1B1 antibodies showed that these antibodies reacted with their corresponding proteins in microsomes prepared from insect cells expressing recombinant human proteins. A single immunoreactive band of 60 kDa was detected by the anti-CYP19 antibody. Similarly, a single immunoreactive band of 56 kDa was detected by the anti-CYP1B1 antibody (Fig. 1B). The specificity of the anti-CYP19 antibody was shown by immunoblot analysis of protein fractions prepared from human placental tissue (Fig. 1C) and immunohistochemistry of human placental tissue (Fig. 1D). Only a single band of approximately 60 kDa was detected in either microsomes (Fig. 1C, lane 1) or the postmitochondrial supernatant (Fig. 1C, lane 2) prepared from two samples of human placenta. Immunohistochemistry demonstrated strong CYP19 staining in the syncytiotrophoblast of the placental villi (Fig. 1D, long arrow), with weaker staining in the cytotrophoblast and decidua (Fig. 1D). The strong staining of CYP19 in the syncytiotrophoblast of the placental villi has been reported for the characterization of other anti-CYP19 antibodies (Esteban et al., 1992). The sensitivity and specificity of the anti-CYP1B1 antibody has been reported previously (Walker et al., 1998;Kim et al., 2004). Representative immunohistochemical analyses of CYP19 and CYP1B1 expression in human breast invasive ductal carcinoma using the purified antibody are shown in Fig. 1C.

Immunohistochemistry of Breast Cancer Using Anti-CYP19 and Anti-CYP1B1 Antibodies

In this study, we evaluated the immunohistochemical expression of CYP19 and CYP1B1 in epithelial cells of breast cancer primarily with IDC. The tissue array we evaluated had 29 cases of IDC, as well as a small number of samples with metastatic carcinoma in lymph node (10

cases), infiltrating lobular carcinoma (two cases), ductal carcinoma in situ (two cases), singlet ring cell carcinoma (one case), solid papillary carcinoma (one case), and medullary carcinoma (one case). Table 1 reports the epithelial cell expression of CYP19 and CYP1B1 in cases of IDC of the breast. The results show a high percentage of expression of both CYP19 and CYP1B1 in epithelium of IDC (22 of 29). Similar results were observed for metastatic carcinoma in lymph node (seven of 10), infiltrating lobular carcinoma (two of two), ductal carcinoma in situ (one of two), singlet ring cell carcinoma (one of one), solid papillary carcinoma (one of one), and medullary carcinoma (one of one) (data not shown). CYP19 was positive in 22 cases of IDC (75.86%). Other tissue compartments (data not shown) expressing CYP19 included the blood vessels (13.79% positive) and fibroblasts (34.48% positive). CYP1B1 was expressed at high frequency and was positive in 28 (96.55%) cases of IDC. Both CYP19 and CYP1B1 were positive in 22 (75.86%) cases. ER, PR, and p53 were positive in 18 (62%), 11 (38%), and 12 (41%) cases, respectively. In addition to the IDC cases, we evaluated 10 samples of metastatic carcinoma in lymph node in epithelium for both CYP19 and CYP1B1 expression. We observed that CYP19 was positively expressed in lymph node in eight (80%) cases, whereas CYP1B1 was positively expressed in nine (90%) cases. Both CYP19 and CYP1B1 expression were positive in 70% cases (data not shown). To determine correlations between immunoreactivity of CYP19, CYP1B1, ER, PR, and p53, statistical analysis, using the Pearson χ^2 test, was used. The correlation between the expression CYP19 and CYP1B1 was 0.33 and was not statistically significant ($p > 0.07$). Furthermore, no statistically significant correlations were found between immunoreactivity for CYP19 and the estrogen receptor, the progesterone receptor, or p53 status. Also, no statistically significant correlations were found using the Fisher's exact test between CYP19 and CYP1B1 (data not shown).

The range of staining intensities of CYP19 and CYP1B1 were assigned scores of 0 to 5 according to the intensity of the staining for the expression of each enzyme. The expression of CYP19 in breast epithelial cells ranged from 0 to 4, with a median value of 1; the expression of CYP1B1 ranged from 0 to 5, with a median value of 3. We also determined the *p* value by Fisher's exact test using staining intensities with the histologic grading 0 to 5 and found no correlation between immunoreactivity of CYP19 and CYP1B1 (data not shown).

Inhibition of Human CYP1B1 Activity by AIs

To explore interactions of CYP1B1 as a potential effector of the disposition of the AIs, the inhibition properties of seven aromatase inhibitors were evaluated for CYP1B1-catalyzed hydroxylation of E2. The chemical structures of steroidal and nonsteroidal aromatase inhibitors are shown in Fig. 2. The inhibition kinetics of steroidal (formestane and exemestane) and nonsteroidal (aminoglutethimide, fadrozole, anastrozole, letrozole, and vorozole) AIs are presented in Fig. 3. None of the AIs tested were potent inhibitors of human CYP1B1, except vorozole. The IC_{50} values for formestane, exemestane, androstenedione, aminoglutethimide, fadrozole, anastrozole, and letrozole for human CYP1B1 E2 4- and 2-hydroxylation were found to be ≥ 100 μM. The IC_{50} values for vorozole for human CYP1B1 E2 4- and 2-hydroxylation were found to be 17 and 21 μM, respectively.

Because of the observed lower IC_{50} values for vorozole compared with other AIs investigated, we determined the K_i value of vorozole. The Dixon plot was used to determine the dissociation constant, K_i, for the binding of inhibitor to enzyme and also to demonstrate the mechanism of inhibition of vorozole (Dixon, 1953). Figure 4, A and B, show Dixon plots for the inhibition of CYP1B1 by vorozole. The intersection of the regression lines in the upper left quadrant of a Dixon plot indicates competitive inhibition. The K_i values of vorozole for E2 4- and 2-hydroxylation by CYP1B1 were found to be 7.26 and 6.84 μM, respectively. It has been reported that for competitive inhibition kinetics, the K_i does not equal to IC_{50} (Cheng and

Prusoff, 1973). We also observed here that IC_{50} and K_i values of vorozole for E2 4- and 2-hydroxylation are different. To provide further unambiguous indication of the type of inhibition, a Cornish-Bowden plot was drawn using the same data (Cornish-Bowden, 1974). We plotted substrate concentration over rate (s/v) versus inhibitor concentration (*i*) at 1 and 5 μM substrate concentrations (Fig. 4, C and D). Linear regression analyses for each of the two substrate concentrations were plotted on a single graph, which is similar to the Dixon plot but complementary to it. It has been suggested that for competitive inhibition, if such lines are drawn, there is no intersection, i.e., the lines are parallel in the plot of s/v against inhibitor concentration. Figure 4, C and D, show similar parallel lines, which further indicate the competitive type of inhibition for vorozole.

Binding of Vorozole to CYP1B1 by Difference Spectroscopy

Addition of vorozole to the microsomal CYP1B1 protein resulted in the formation of a type II binding spectrum (Fig. 5). Addition of varying concentrations of vorozole resulted in a progressive spectral change. The spectral change was characterized by the appearance of an absorption peak at about 422 nm, a trough at about 390 nm, and an isosbestic point at about 410 nm.

Discussion

Here, we report the production and characterization of a specific antibody raised against hexahistidine-tagged fusion protein of CYP19 that was produced and purified from *E. coli*. The expressions of CYP19 and CYP1B1 in cases of breast cancer were studied by immunohistochemical analysis. These analyses showed that a high percentage (76%) of the cases of IDC of the breast expressed both enzymes in the ductal epithelium. However, statistical analysis showed no significant correlation between the immunohistochemical expression of CYP19 and CYP1B1; the observed correlation was 0.33 ($p > 0.07$). Other characteristics of the tumor such as ER, PR, and p53 status did not show any statistically significant correlation with tumor aromatase. It should be noted that the number of cases of IDC evaluated in this study was small ($n = 29$). A recent paper in a population based study ($n = 698$) on hormonal markers in breast cancer identified a significant correlation ($p < 0.01$, Pearson correlation coefficient = 0.14) between CYP19 and CYP1B1 (Yang et al., 2007). We believe that the likely reason for the difference in results between this study and ours is sample size, with the larger study (Yang et al., 2007) having greater power to detect this correlation. In another study (Esteban et al., 1992), a significant ($p = 0.04$), but inverse correlation between CYP19 and ER immunoreactivity was reported, indicating a likelihood of detecting CYP19 in ER-negative tumors. A significant correlation between the expression of cyclooxygenase-2 and CYP19 in IDC and ductal carcinoma in situ from the same breast has also been reported (Oliveira et al., 2006). This group reported that 70% of the samples stained positive for CYP19 enzyme expression. In a recent study, two new CYP19 monoclonal antibodies were described and validated in an analysis of 43 cases of IDC (Sasano et al., 2005). Importantly, this latter study (Sasano et al., 2005) showed that there was a significant positive correlation between biochemical activity and CYP19 immunopositivity only in malignant epithelium.

CYP1B1 protein is overexpressed in malignant tumors of the breast (McFadyen et al., 1999). Interestingly, the elevated expression of CYP1B1 protein in breast cancer tissues has recently been shown to be regulated by micro-RNA (miRNA) expression (Tsuchiya et al., 2006). The researchers found that there was a significant inverse association between the expression levels of a specific miRNA (miR-27b) and CYP1B1 protein. It has been suggested that decreased expression of miR-27b would be one of the causes of the high expression of CYP1B1 protein in cancerous tissues. To our knowledge, the potential influence of miRNAs on the expression of CYP19 protein in tumor tissues has not been investigated.

As an approach to evaluate CYP1B1 as a potential determinant of the disposition of AIs, we determined the inhibition properties of a series of AIs against CYP1B1-catalyzed hydroxylation of E2. Instead of measuring metabolites of each compound, we screened the AIs for inhibition of CYP1B1 because competitive inhibitors may also be enzyme substrates. Of the seven compounds tested, only vorozole, a triazole derivative, exhibited potent inhibition of human CYP1B1 activity. The other AIs studied, formestane, exemestane, aminoglutethimide, fadrozole, anastrozole, and letrozole, showed only weak inhibition of the catalytic activity of CYP1B1. The Dixon and Cornish-Bowden plots indicate that there is a competitive part in the inhibition of the human CYP1B1 enzyme by vorozole. Previously, this compound has been reported as a competitive inhibitor of aromatase (Montellano, 1995). Although vorozole inhibits human CYP1B1, this compound is over 1000-fold more active for aromatase inhibition (Wouters et al., 1994). It is unclear why other nonsteroidal inhibitors were not found to be as effective as vorozole in decreasing the catalytic activity of CYP1B1. These differences of action on CYP1B1 by nonsteroidal inhibitors may be due to the differences in their chemical structures. Although the inhibitory activities of AIs against human CYP1B1 have not been previously studied, the effect of tamoxifen, a nonestradiol antiestrogen and a chemopreventive agent widely used for breast cancer treatment, was tested against human CYP1B1 as a possible inhibitor. However, the results of these studies were inconsistent (Rochat et al., 2001; Sridar et al., 2002). Rochat et al. (2001) have reported that tamoxifen reversibly inhibits CYP1B1 and is a noncompetitive inhibitor. However, in another independent study, Sridar et al. (2002) mentioned that tamoxifen had no effect on the activities of CYP1B1.

The binding of vorozole to human CYP1B1 resulted in type II spectra (Fig. 5), which indicates that this compound is likely associated with ligation of the heme iron (Miller, 2006). It has been reported that this type of binding arises from the nitrogen interaction with the iron atom. The chemical structures of type II compounds usually possess atoms with freely accessible nonbonding electrons, such as nitrogen lone pair or aromatic and aliphatic amines (Schenkman et al., 1967;Miller, 2006). It is to be noted that vorozole, a nonsteroidal type II inhibitor, like other nonsteroidal compounds, has basic nitrogen atoms that allows the inhibitors to interact reversibly with the heme prosthetic group, a common feature of all cytochrome P450 enzymes (Johnston and Dowsett, 2003). Thus, vorozole is unlikely to be a substrate for CYP1B1. Preliminary studies with microsomal incubation of CYP1B1 with vorozole indicate no metabolic products as determined by high-performance liquid chromatography with UV/Vis (data not shown).

AIs have been proposed for the prevention of breast cancer. In adjuvant therapy trials comparing tamoxifen with AIs, the reduction of contralateral breast cancer is 50% greater with the AI than with tamoxifen in separate trials (Kudachadkar and O'Regan, 2005). It has been postulated that the greater efficacy of the AIs is because of the reduction of estrogen levels and therefore their genotoxic metabolites. Vorozole reduced plasma levels of E2 in premenopausal women to ~36% after 8 h of intake (Wouters et al., 1989). It was also a more effective estrogen suppressant, resulting in 30% more suppression of serum E2 levels in postmenopausal women than formestane, a steroidal inhibitor (Dowsett et al., 1999). However, vorozole has not been approved for use by the U.S. Food and Drug Administration, although its clinical activity was similar to anastrazole and letrozole in phase III trials (Hamilton and Piccart, 1999). It has been reported that at clinically administered doses, the plasma half-lives of anastrozole (1 mg/day), letrozole (2.5 mg/day), and exemestane (25 mg/day) are 41 to 48 h, 2 to 4 days, and 27 h, respectively (Buzdar, 2003). There are some differences in the degree of plasma estradiol suppression among the 3rd generation AIs. The three aromatase inhibitors anastrozole, letrozole, and exemestane, that are currently approved by the Food and Drug Administration for use in breast cancer treatment, decrease estradiol by 84.9, 87.8, and 92.2%, respectively (Osborne and Tripathy, 2005). The 3rd generation AIs are well tolerated and suppress endogenous estrogen levels in postmenopausal women, but estrogen deficiency is one of the

most important factors for the pathogenesis of osteoporosis. Osteoporotic fractures and greater bone mineral loss are typically more associated with AIs (Osborne and Tripathy, 2005). Based on the results of this study, it is indicated that with the exception of vorozole, the AIs are specific for aromatase relative to CYP1B1, a cytochrome P450 widely expressed in breast tissue and responsible for estrogen metabolism. Overall, the results of this study indicate that CYP1B1 is not a major determinant of the disposition of AIs.

Acknowledgements

We thank William R. Miller for providing the aromatase inhibitors and valuable comments in the preparation of the manuscript. We also thank Kimberly Reid and Monali Master for assistance with microsomes preparation and Jennifer Tzefakes and Lou Boykins of the Integrated Microscopy Center for technical support with immunohistochemistry.

This study was supported by the National Institutes of Health (Grant ES 08148), by the Department of Defense (Grant DAMD 17-03-1-0229), and by the W. Harry Feinstone Center for Genomic Research.

ABBREVIATIONS

AI
: aromatase inhibitor

E2
: 17β-estradiol

PAGE
: polyacrylamide gel electrophoresis

IDC
: invasive ductal carcinoma

ER
: estrogen receptor

PR
: progesterone receptor

miRNA
: micro-RNA

4-OHE2
: 4-hydroxy estradiol

2-OHE2
: 2-hydroxy estradiol

References

Aoyama T, Korzekwa K, Nagata K, Gillette J, Gelboin HV, Gonzalez FJ. Estradiol metabolism by complementary deoxyribonucleic acid-expressed human cytochrome P450s. Endocrinology 1990;126:3101–3106. [PubMed: 2161748]

Brodie A, Lu Q, Nakamura J. Aromatase in the normal breast and breast cancer. J Steroid Biochem Mol Biol 1997;61:281–286. [PubMed: 9365202]

Bulun SE, Price TM, Aitken J, Mahendroo MS, Simpson ER. A link between breast cancer and local estrogen biosynthesis suggested by quantification of breast adipose tissue aromatase cytochrome P450 transcripts using competitive polymerase chain reaction after reverse transcription. J Clin Endocrinol Metab 1993;77:1622–1628. [PubMed: 8117355]

Buzdar AU. Pharmacology and pharmacokinetics of the newer generation aromatase inhibitors. Clin Cancer Res 2003;9:468S–472S. [PubMed: 12538502]

Cavalieri E, Chakravarti D, Guttenplan J, Hart E, Ingle J, Jankowiak R, Muti P, Rogan E, Russo J, Santen R, et al. Catechol estrogen quinones as initiators of breast and other human cancers: implications for biomarkers of susceptibility and cancer prevention. Biochim Biophys Acta 2006;1766:63–78. [PubMed: 16675129]

Cheng YC, Prusoff WH. Relationship between the inhibition constant (K_I) and the concentration of inhibitor which causes 50 percent inhibition (I_{50}) of an enzymatic reaction. Biochem Pharmacol 1973;22:3099–3108. [PubMed: 4202581]

Corbin CJ, Graham-Lorence S, McPhaul M, Mason JI, Mendelson CR, Simpson ER. Isolation of a full-length cDNA insert encoding human aromatase system cytochrome P-450 and its expression in nonsteroidogenic cells. Proc Natl Acad Sci U S A 1988;85:8948–8952. [PubMed: 2848247]

Cornish-Bowden A. A simple graphical method for determining the inhibition constants of mixed, uncompetitive and non-competitive inhibitors. Biochem J 1974;137:143–144. [PubMed: 4206907]

Dixon M. The determination of enzyme inhibitor constants. Biochem J 1953;55:170–171. [PubMed: 13093635]

Dowsett M, Doody D, Miall S, Howes A, English J, Coombes RC. Vorozole results in greater oestrogen suppression than formestane in postmenopausal women and when added to goserelin in premenopausal women with advanced breast cancer. Breast Cancer Res Treat 1999;56:25–34. [PubMed: 10517340]

Esteban JM, Warsi Z, Haniu M, Hall P, Shively JE, Chen S. Detection of intratumoral aromatase in breast carcinomas: an immunohistochemical study with clinicopathologic correlation. Am J Pathol 1992;140:337–343. [PubMed: 1739127]

Hamilton A, Piccart M. The third-generation non-steroidal aromatase inhibitors: a review of their clinical benefits in the second-line hormonal treatment of advanced breast cancer. Ann Oncol 1999;10:377–384. [PubMed: 10370778]

Hayes CL, Spink DC, Spink BC, Cao JQ, Walker NJ, Sutter TR. 17β-Estradiol hydroxylation catalyzed by human cytochrome P450 1B1. Proc Natl Acad Sci U S A 1996;93:9776–9781. [PubMed: 8790407]

Jefcoate CR, Liehr JG, Santen RJ, Sutter TR, Yager JD, Yue W, Santner SJ, Tekmal R, Demers L, Pauley R, et al. Tissue-specific synthesis and oxidative metabolism of estrogens. J Natl Cancer Inst Monogr 2000;27:95–112. [PubMed: 10963622]

Joensuu H, Ejlertsen B, Lonning PE, Rutqvist LE. Aromatase inhibitors in the treatment of early and advanced breast cancer. Acta Oncol 2005;44:23–31. [PubMed: 15848903]

Johnston SR, Dowsett M. Aromatase inhibitors for breast cancer: lessons from the laboratory. Nat Rev Cancer 2003;3:821–831. [PubMed: 14668813]

Kim JH, Sherman ME, Curriero FC, Guengerich FP, Strickland PT, Sutter TR. Expression of cytochromes P450 1A1 and 1B1 in human lung from smokers, non-smokers, and ex-smokers. Toxicol Appl Pharmacol 2004;199:210–219. [PubMed: 15364538]

Kudachadkar R, O'Regan RM. Aromatase inhibitors as adjuvant therapy for postmenopausal patients with early stage breast cancer. CA Cancer J Clin 2005;55:145–163. [PubMed: 15890638]

Liehr JG, Ricci MJ. 4-Hydroxylation of estrogens as marker of human mammary tumors. Proc Natl Acad Sci U S A 1996;93:3294–3296. [PubMed: 8622931]

Lu Q, Nakmura J, Savinov A, Yue W, Weisz J, Dabbs DJ, Wolz G, Brodie A. Expression of aromatase protein and messenger ribonucleic acid in tumor epithelial cells and evidence of functional significance of locally produced estrogen in human breast cancers. Endocrinology 1996;137:3061–3068. [PubMed: 8770932]

McFadyen MC, Breeman S, Payne S, Stirk C, Miller ID, Melvin WT, Murray GI. Immunohistochemical localization of cytochrome P450 CYP1B1 in breast cancer with monoclonal antibodies specific for CYP1B1. J Histochem Cytochem 1999;47:1457–1464. [PubMed: 10544218]

Miki Y, Suzuki T, Tazawa C, Yamaguchi Y, Kitada K, Honma S, Moriya T, Hirakawa H, Evans DB, Hayashi S, et al. Aromatase localization in human breast cancer tissues: possible interactions between intratumoral stromal and parenchymal cells. Cancer Res 2007;67:3945–3954. [PubMed: 17440110]

Miller WR. Aromatase and the breast: regulation and clinical aspects. Maturitas 2006;54:335–341. [PubMed: 16730141]

Miller WR. Aromatase activity in the breast tissue. J Steroid Biochem Mol Biol 1991;39:783–790. [PubMed: 1954167]

Montellano, PRO. Cytochrome P450 Structure, Mechanism, and Biochemistry. 2. Plenum Press; New York: 1995.

Muskhelishvili L, Thompson PA, Kusewitt DF, Wang C, Kadlubar FF. In situ hybridization and immunohistochemical analysis of cytochrome P450 1B1 expression in human normal tissues. J Histochem Cytochem 2001;49:229–236. [PubMed: 11156691]

Oliveira VM, Piato S, Silva MA. Correlation of cyclooxygenase-2 and aromatase immunohistochemical expression in invasive ductal carcinoma, ductal carcinoma in situ, and adjacent normal epithelium. Breast Cancer Res Treat 2006;95:235–241. [PubMed: 16322898]

Osborne C, Tripathy D. Aromatase inhibitors: rationale and use in breast cancer. Annu Rev Med 2005;56:103–116. [PubMed: 15660504]

Rahman M, Sutter CH, Emmert GL, Sutter TR. Regioselective 2-hydroxylation of 17β-estradiol by rat cytochrome P4501B1. Toxicol Appl Pharmacol 2006;216:469–478. [PubMed: 16893557]

Rochat B, Morsman JM, Murray GI, Figg WD, Mcleod HL. Human CYP1B1 and anticancer agent metabolism: mechanism for tumor-specific drug inactivation? J Pharmacol Exp Ther 2001;296:537–541. [PubMed: 11160641]

Sasano H, Anderson TJ, Silverberg SG, Santen RJ, Conway M, Edwards DP, Krause A, Bhatnagar AS, Evans DB, Miller WR. The validation of new aromatase monoclonal antibodies for immunohistochemistry-a correlation with biochemical activities in 46 cases of breast cancer. J Steroid Biochem Mol Biol 2005;95:35–39. [PubMed: 16024247]

Schenkman JB, Remmer H, Estabrook RW. Spectral studies of drug interaction with hepatic microsomal cytochrome. Mol Pharmacol 1967;3:113–123.

Shimada T, Hayes CL, Yamazaki H, Amin S, Hecht SS, Guengerich FP, Sutter TR. Activation of chemically diverse procarcinogens by human cytochrome P-4501B1. Cancer Res 1996;56:2979–2984. [PubMed: 8674051]

Singh S, Chakravarti D, Edney JA, Hollins RR, Johnson PJ, West WW, Higginbotham SM, Cavalieri EL, Rogan EG. Relative imbalances in the expression of estrogen-metabolizing enzymes in the breast tissue of women with breast carcinoma. Oncol Rep 2005;14:1091–1096. [PubMed: 16142378]

Sridar C, Kent UM, Notley LM, Gillam EMJ, Hollenberg PF. Effect of tamoxifen on the enzymatic activity of human cytochrome CYP2B6. J Pharmacol Exp Ther 2002;301:945–952. [PubMed: 12023523]

Sutter TR, Tang YM, Hayes CL, Wo YY, Jabs EW, Li X, Yin H, Cody CW, Greenlee WF. Complete cDNA sequence of a human dioxin-inducible mRNA identifies a new gene subfamily of cytochrome P450 that maps to chromosome 2. J Biol Chem 1994;69:13092–13099. [PubMed: 8175734]

Tsuchiya Y, Nakajima M, Takagi S, Taniya T, Yokoi T. MicroRNA regulates the expression of human cytochrome P4501B1. Cancer Res 2006;66:9090–9098. [PubMed: 16982751]

Walker NJ, Crofts FG, Li Y, Lax SF, Hayes CL, Strickland PT, Lucier GW, Sutter TR. Induction and localization of cytochrome P450 1B1 (CYP1B1) protein in the livers of TCDD-treated rats: detection using polyclonal antibodies raised to histidine-tagged fusion proteins produced and purified from bacteria. Carcinogenesis 1998;19:395–402. [PubMed: 9525272]

Wouters W, Coster RD, Tuman RW, Bowden CR, Bruynseels J, Vanderpas H, Van Rooy P, Amery WK, Janssen PA. Aromatase inhibition by R 76713: experimental and clinical pharmacology. J Steroid Biochem 1989;34:427–430. [PubMed: 2696850]

Wouters W, Snoeck E, Coster RD. Vorozole, a specific non-steroidal aromatase inhibitors. Breast Cancer Res Treat 1994;30:89–94. [PubMed: 7726994]

Yang XR, Pfeiffer RM, Garcia-Closas M, Rimm DL, Lissowska J, Brinton LA, Peplonska B, Hewitt SM, Cartun R, Mandich D, et al. Hormonal markers in breast cancer: co-expression, relationship with pathologic characteristics and risk factor associations in a population-based study. Cancer Res 2007;67:10608–10617. [PubMed: 17968031]

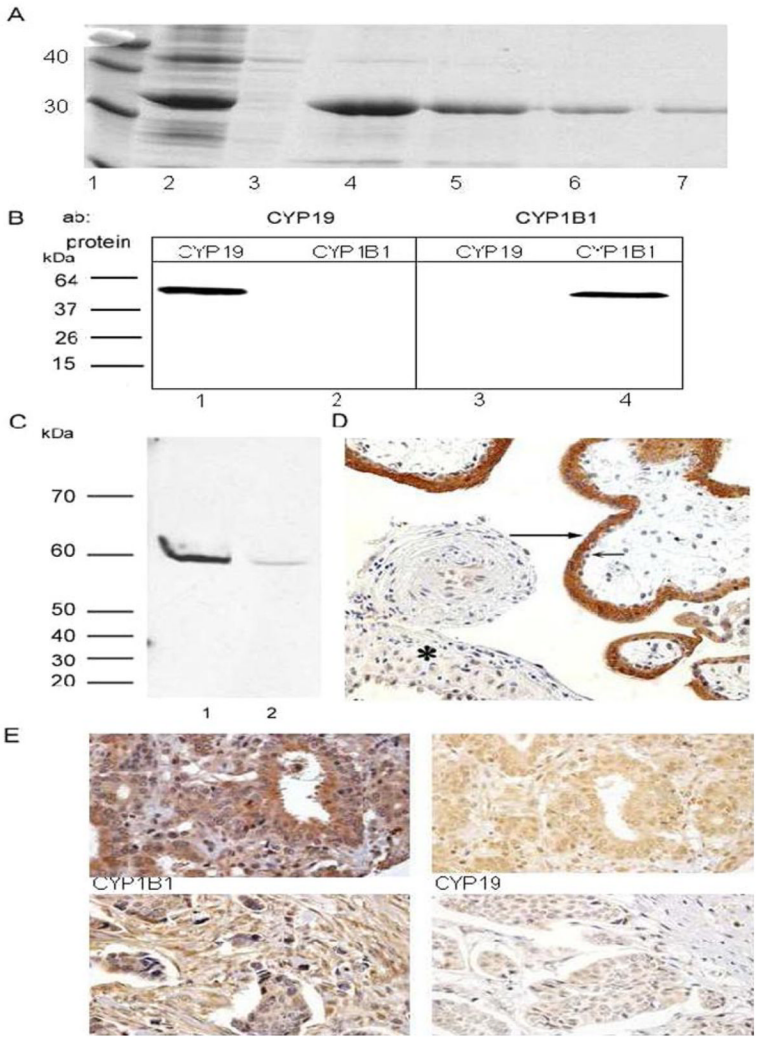

Fig. 1.

Expression of CYP19 and CYP1B1 in human breast invasive ductal carcinoma. A, expression and purification of His_6-CYP19 fusion protein from *E. coli*. Protein samples were fractionated on a 12% SDS-PAGE and stained with Coomassie Blue. Lane 1, molecular mass standards (kilodaltons); lane 2, induced *E. coli* cultures (15 μl of cell lysate was loaded as described under *Materials and Methods*); lane 3, uninduced *E. coli* cultures; lane 4 to 7, fractions of fusion protein purified by nickel-chelate affinity chromatography. B, immunoblots of CYP19 and CYP1B1. Lane 1 and 3, 1 pmol recombinant CYP19 microsomes from BD Gentest; lane 2 and 4, 1 pmol recombinant CYP1B1 microsomes from BD Gentest. C, immunoblot of CYP19 in fractions of human placental tissue (1:2000 dilution of anti-CYP19 antibody). Lane 1, 100 μg of microsomal protein from placenta B; lane 2, 100 μg of postmitochondrial supernatant from placenta. C and D, immunohistochemical analysis of CYP19 expression in placental tissue. CYP19 is strongly expressed in the syncytiotrophoblast of the placental villi (long arrow) and weakly expressed in the cytotrophoblast (short arrow) and decidua (asterisk). Photograph, magnification, ×200. E, immunohistochemical analyses of CYP1B1 (left) and CYP19 (right) expression in human breast cancer (invasive ductal carcinoma) samples. The upper panels are immunostained sample from the same individual in the same region. The lower panels are immunostained sample from another individual in the same region. Photographs, magnification, ×400.

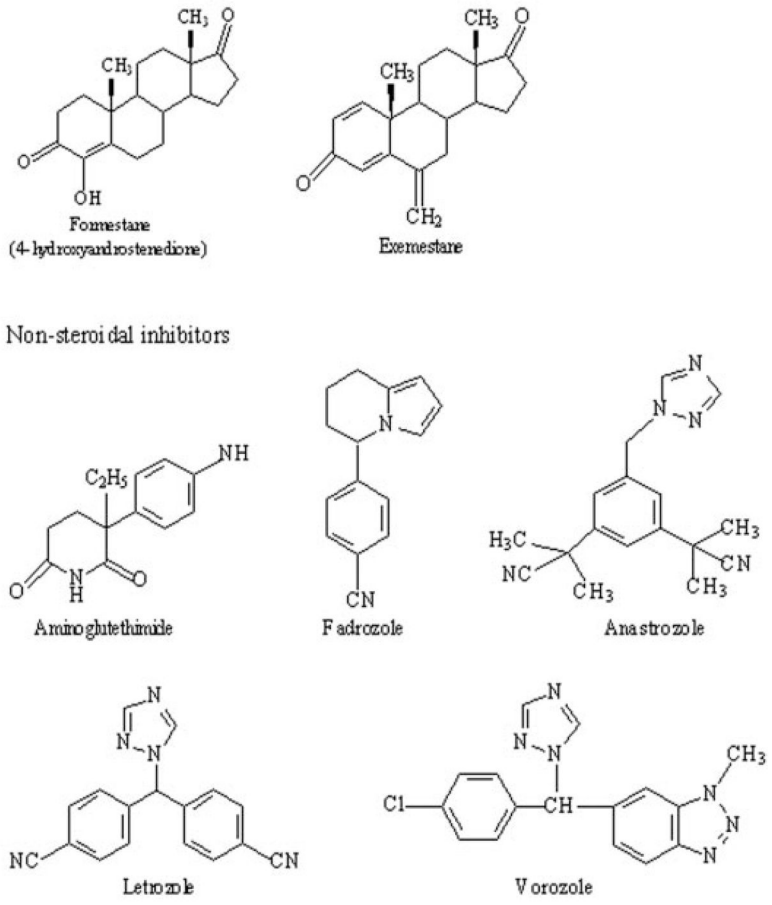

Fig. 2.
Chemical structures of seven aromatase inhibitors. Steroidal inhibitors, formestane and exemestane; nonsteroidal inhibitors, aminoglutethimide, fadrozole, anastrozole, letrozole, and vorozole.

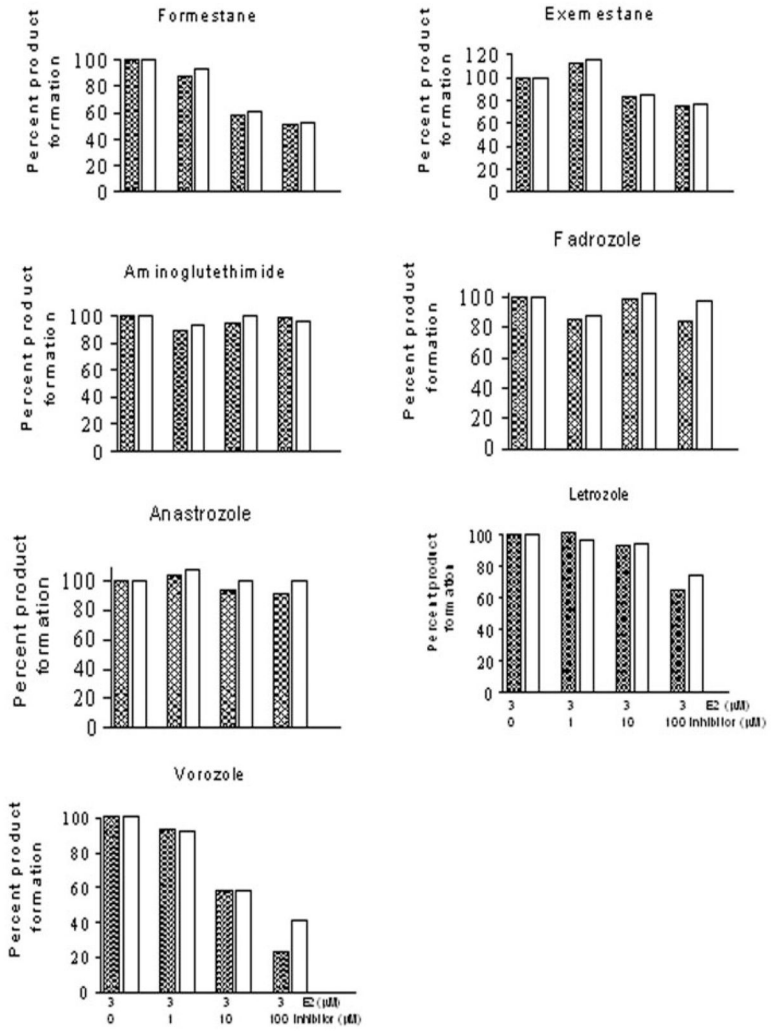

Fig. 3.

Inhibition of human CYP1B1 by aromatase inhibitors. Microsomes containing 10 pmol CYP1B1 were incubated with 3 μM E2 and 0.0, 1.0, 10.0, and 100 μM each aromatase inhibitors in a single determination. Reactions were run for 15 min at 37°C, and rates of 4-OHE2 (hatched bar) and 2-OHE2 (open bar) formation were determined as described under *Materials and Methods*.

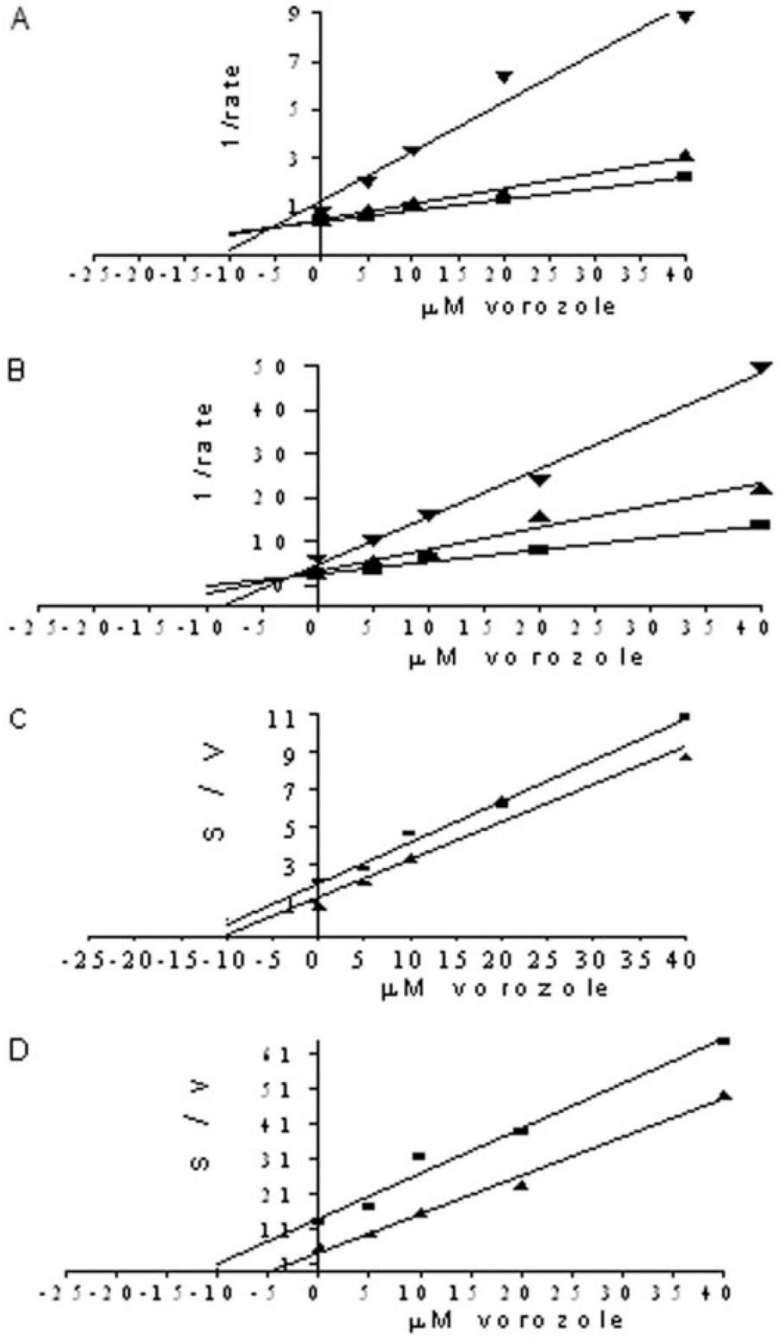

Fig. 4.

Determination of K_i values and type of inhibition. A and B, Dixon plots for the inhibition of human CYP1B1 by vorozole. The inhibitor was tested in single determination at five concentrations in the presence of 1, 3, and 5 μM E2. The reactions contained 10 pmol CYP1B1 and were run for 15 min at 37°C. A, human CYP1B1 (4-OHE2); B, human CYP1B1 (2-OHE2). ▼, 1 μM; ▲, 3 μM; ■, 5 μM E2. C and D, Cornish-Bowden plots for the inhibition of human CYP1B1 by vorozole. The plots were constructed using the same data. C, human CYP1B1 (4-OHE2); D, human CYP1B1 (2-OHE2). ▲, 1 μM; ■, 5 μM E2.

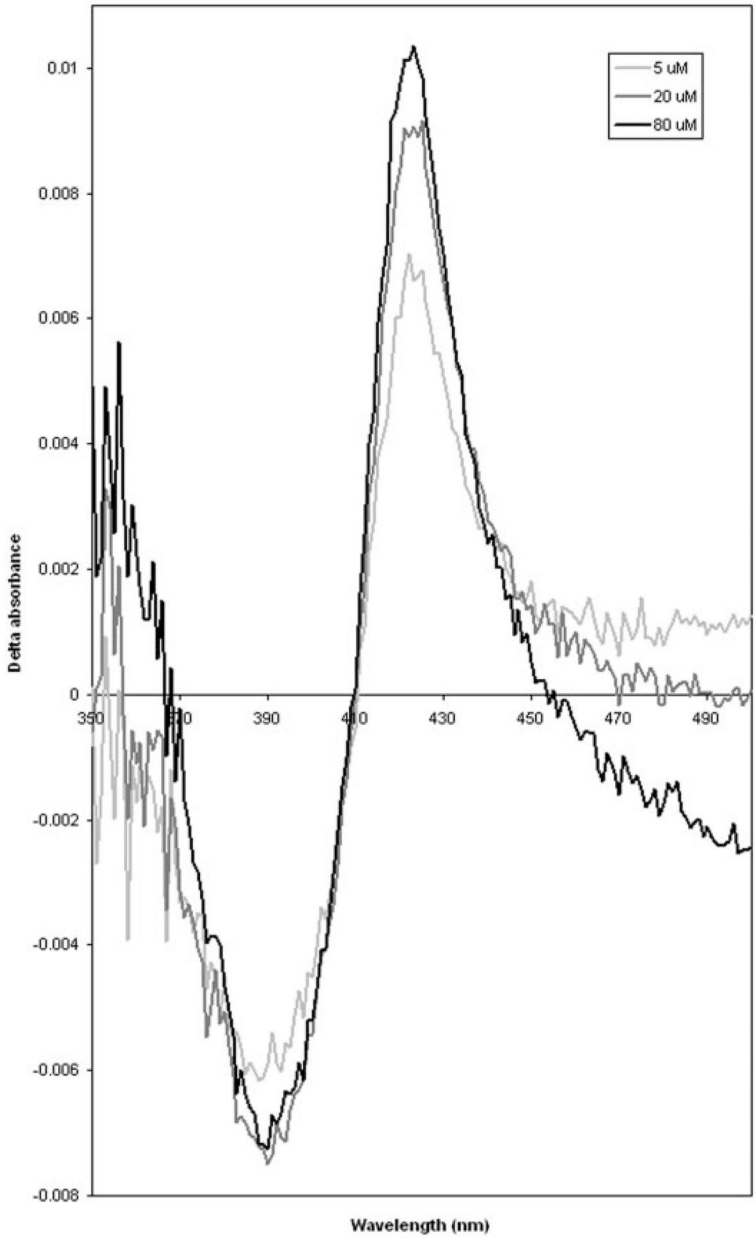

Fig. 5.

Binding spectra of vorozole to human CYP1B1 expressed in yeast. Microsomal protein (1 mg/ml) was suspended in 0.1 M KPO_4 buffer, pH 7.4, and placed in two cuvettes. The difference spectrum was obtained by adding vorozole to a final concentration of 5.0, 20.0, and 80.0 μM dissolved in dimethyl sulfoxide in the sample cuvette, and an equal volume of carrier solvent was added to the reference cuvette.

TABLE 1

Summary of statistical analysis of epithelial cell expression of CYP19 and CYP1B1 in invasive ductal carcinoma of the breast

	Aromatase Negative	Aromatase Positive	Total	*p* Value*	Correlation Coefficient
CYP1B1					
Negative	1	0	1	0.0712	0.33503
Positive	6	22	28		
ER					
Negative	3	8	11	0.7578	0.05727
Positive	4	14	18		
PR					
Negative	4	14	18	0.7578	−0.05727
Positive	3	8	11		
p53					
Negative	4	13	17	0.9274	−0.01693
Positive	3	9	12		

*Analysis by the Pearson χ^2 test.